

# ATTITUDE SENSOR PSEUDONOISE\*

Joseph A. Hashmall  
Scott E. Lennox  
a.i.solutions, Inc.  
joseph.hashmall@ai-solutions.com

## ABSTRACT

Even assuming perfect attitude sensors and gyros, sensor measurements on a vibrating spacecraft have apparent errors. These apparent sensor errors, referred to as pseudonoise, arise because gyro and sensor measurements are performed at discrete times. This paper explains the concept of pseudonoise, quantifies its behavior, and discusses the effect of vibrations that are nearly commensurate with measurement periods. Although pseudonoise does not usually affect attitude determination it does affect sensor performance evaluation.

Attitude rates are usually computed from differences between pairs of accumulated angle measurements at different times and are considered constant in the periods between measurements. Propagation using these rates does not reproduce exact instantaneous spacecraft attitudes except at the gyro measurement times. Exact sensor measurements will therefore be inconsistent with estimates based on the propagated attitude. This inconsistency produces pseudonoise.

The characteristics of pseudonoise were determined using a simple, one-dimensional model of spacecraft vibration. The statistical properties of the deviations of measurements from model truth were determined using this model and a range of different periods of sensor and rate measurements.

This analysis indicates that the magnitude of pseudonoise depends on the ratio of the spacecraft vibration period to the time between gyro measurements and can be as much as twice the amplitude of the vibration. In cases where the vibration period and gyro or sensor measurement period are nearly commensurate, unexpected changes in pseudonoise occur.

\* This work was supported by the National Aeronautics and Space Administration (NASA) / Goddard Space Flight Center (GSFC), Greenbelt, MD, USA, Contract NNG04DA01C.

## INTRODUCTION

Assume that a spacecraft vibrates with a known frequency and amplitude. The model used here contains three features:

- True sinusoidal angular displacements of unit amplitude and unit frequency. The angular displacements are sinusoidal.
- Exact measurements of the angular displacement by two sensors. Sensor displacement measurements are defined by their cadence (number of measurements made in one vibration period) and a phase of the first displacement measurement used.
- Exact rate measurements by an integrating rate sensor. This sensor provides integrated rates from one rate measurement to the next at a rate sensor cadence and starting at an initial phase. It is assumed that the integrated rate at the time of each rate measurement is exactly equal to the true angular displacement at that time. Displacements are estimated from rate measurements by interpolation or extrapolation.
  - Interpolated rates are most often used in post-processing when all of the data is available before processing. In this case, the estimate of the displacement angle at any time is obtained by linear interpolation of the integrated rates before and after the time.
  - Extrapolated rates are most often used in real time processing when data is processed in the order in which it is generated. In this case, the estimate of the displacement angle at any time is obtained by linear extrapolation of the two most recent integrated rate measurements.

Attitude estimation filters which use rate data attempt to minimize the differences between the measured displacement and the displacement estimated (by interpolation or extrapolation) from the rate measurements.

Even with exact measurements, true spacecraft vibrations cause an apparent noise in the attitude sensor. This noise is referred to as pseudonoise. The present paper describes the origin and properties of pseudonoise. It arises because the linear interpolation or extrapolation used to estimate displacements is not exact.

Figure 1 illustrates the origin of pseudonoise. In it, the sinusoidal line represents the true angular displacement of the spacecraft in one dimension. On the sinusoidal line are circles representing rate sensor measurements of integrated displacements since the previous measurements. Xs on the sinusoidal line represent attitude sensor measurements of the angular displacements. All of the measurements are exactly on the line because sensors are assumed to have no error.

At times other than those of rate measurements, the displacement is obtained either by interpolation (in the case of post-hoc batch least-squares (BLS) estimators), or by extrapolation (in the case of real-time filters). At the time of the displacement measurement (X), the extrapolated or interpolated displacement differs from the true measured displacement by a significant amount. This difference is pseudonoise. It arises solely from the fact that the function used to interpolate or extrapolate rate measurements (linear in this case) cannot reproduce the true spacecraft displacement between measurements.

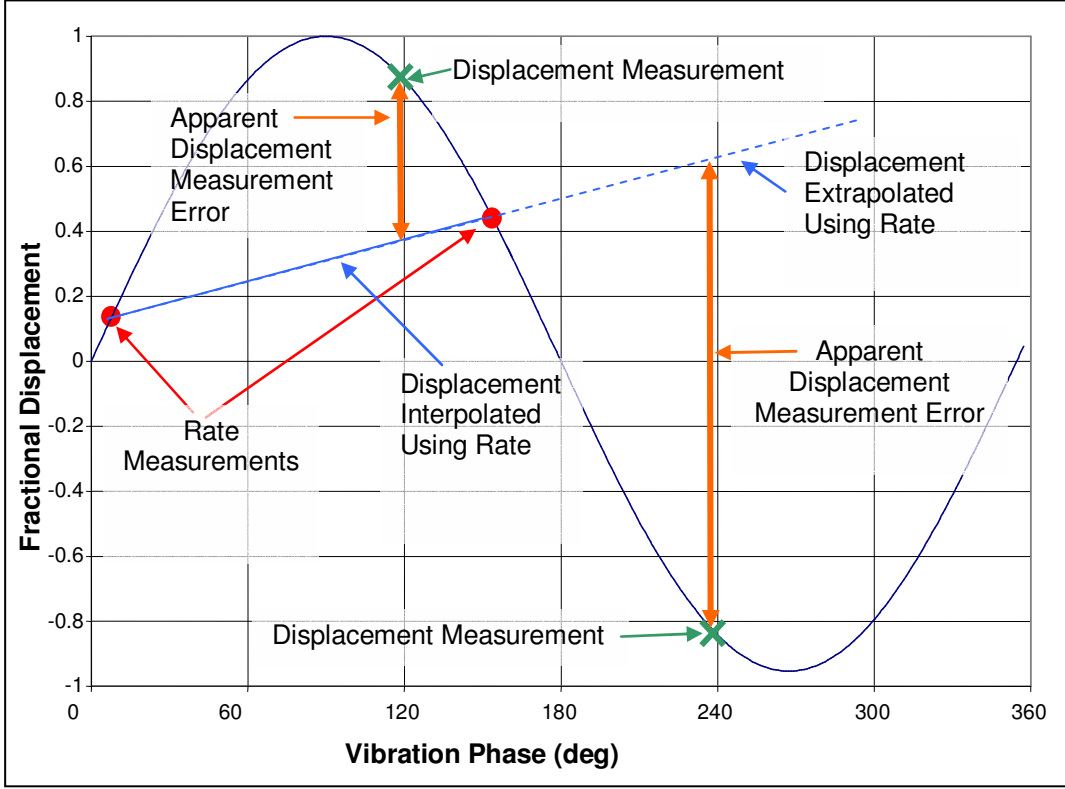


**Figure 1. Illustration of Pseudonoise**

## CHARACTERIZATION OF PSEUDONoise

All of the descriptions of pseudonoise in this paper shall be related to a sinusoidal vibration of unit frequency and unit amplitude. Pseudonoise magnitudes are linear with vibration amplitude. Characteristics that depend on the vibration frequency can be equivalently viewed as depending on the rate measurement cadence—the number of rate measurements that are made in a single vibration period.

It is assumed that the rate measurements and displacement measurements are independent and exact. Attitude sensor measurements are modeled as the exact displacements at each time. Rate measurements are constructed from pairs of exact displacement measurements with rates assumed to be constant between these displacement measurements. This assumption produces results equivalent to those from a perfect Kalman filter, with zero sensor weight, starting from an exact initial attitude.

In a simple, 1-dimensional model, the spacecraft vibration may be represented as a periodic angular displacement described by:

$$\theta_\phi = \sin(\phi) \quad (1)$$

where  $\phi$  is the phase at which the displacement,  $\theta$ , occurs. In the notation used here, the phase,  $\phi$ , is not limited to  $2\pi$ , but increases without limit. Pseudonoise is given in terms of the

measurement phase,  $\phi_m$ , and phases of the two rate measurements,  $\phi_0$  and  $\phi_1$ , that are used to compute the expected displacement, by:

$$p_{\phi m} = \theta_m - \theta_{m, \text{expected}} \quad (2)$$

where

$$\theta_m = \sin(\phi_m) \quad (3)$$

$$\theta_{m, \text{expected}} = \theta_1 + \frac{(\theta_1 - \theta_0)}{(\phi_1 - \phi_0)} (\phi_m - \phi_1) \quad (4)$$

Note that for interpolation,  $\phi_0 \leq \phi_m \leq \phi_1$ ; whereas, for extrapolation, it is assumed that  $(2\phi_1 - \phi_0) \geq \phi_m \geq \phi_1$ .

It is clear from Figure 1 that pseudonoise depends strongly on the cadence of the rate measurements. The high and low rate limits are considered next.

### High Rate Cadence

As the cadence becomes large, the approximation of the rate by linear interpolation or extrapolation becomes more accurate, and the pseudonoise becomes small. This is the case for very low frequency vibrations or very high frequency rate measurements. As  $\phi_0$  approaches  $\phi_1$ :

$$\frac{(\theta_1 - \theta_0)}{(\phi_1 - \phi_0)} \cong \frac{d\theta}{d\phi} \quad (5)$$

and

$$\theta_{m, \text{expected}} \cong \theta_m \quad (6)$$

so the pseudonoise approaches zero, Rate measurements follow the vibration well and pseudonoise is negligible. This case is illustrated in Figure 2.

### Low Rate Cadence

As the cadence becomes small, there are many complete vibrations between any adjacent pairs of rate measurements. In this case, the vibration is at a high frequency compared to the rate measurements. As seen in Figure 3, rate measurements are bounded by the vibration amplitude divided by the relatively long time between measurements. The calculated rates therefore tend to be small compared to those in the high rate cadence case.

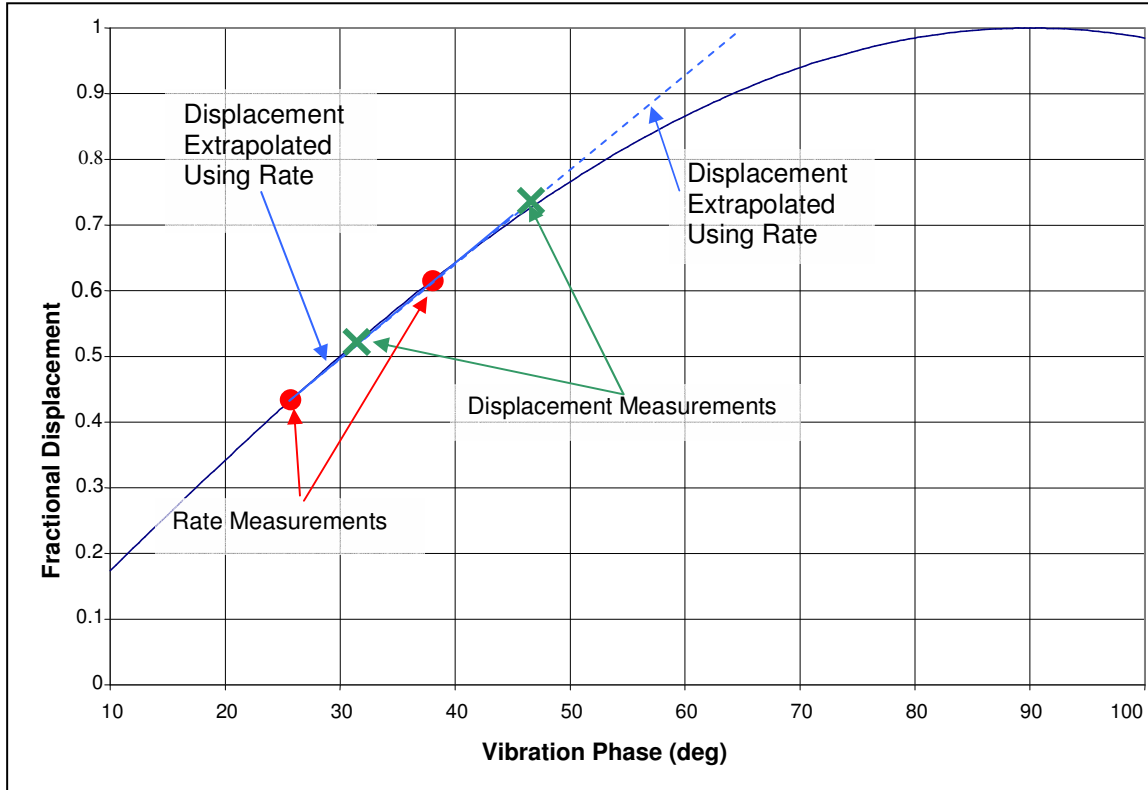


**Figure 2. Pseudonoise with High Rate Cadence (Low Vibration Frequency)**

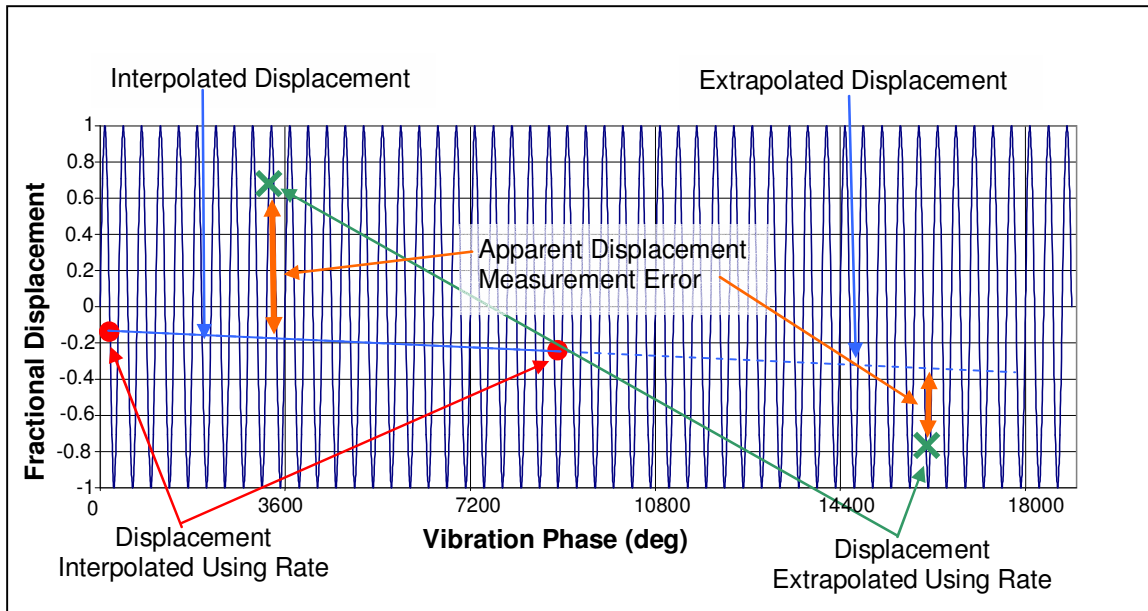


**Figure 3. Pseudonoise with Low Rate Cadence (High Vibration Frequency)**

In the low rate cadence case, the phase of the displacement measurement can be considered to be independent of the phase of the rate measurements. The displacements  $\theta_m$  and

$\theta_{m,expected}$  (in Eq. (2)) are uncorrelated, and the uncertainty of their difference is just the root-sum-square of the uncertainty of the two terms.

The standard deviation of  $\theta_m$  is given by:

$$\sigma_{\theta_m} = \sqrt{\frac{\sum \sin^2 \phi_m}{n-1}} \cong \sqrt{\frac{\int \sin^2 \phi_m d\phi_m}{\int d\phi_m}} = \frac{1}{\sqrt{2}} \quad (7)$$

where the summation is over a large set of  $n$  measurements spanning many vibration periods and the integration is over continuous measurements in a single vibration period.

The standard deviation of  $\theta_{m,expected}$  depends on the phases of the two rate measurements. These phases,  $\phi_0$  and  $\phi_1$ , can be equivalently represented by  $\phi_0$  and  $\Delta\phi$  ( $\Delta\phi = \phi_1 - \phi_0$ ). Displacement  $\theta_{m,expected}$  lies on a straight line between the points  $[\phi_0, \sin\phi_0]$  and  $[\phi_1, \sin\phi_1]$ . Its standard deviation has been calculated for values of  $\phi_0$  between 0 and 360 deg and of  $\Delta\phi$  between 360 to 720 deg. The results are shown in Figure 4. The form of the surface shown is similar for any complete 360 degree cycle of  $\Delta\phi$ .

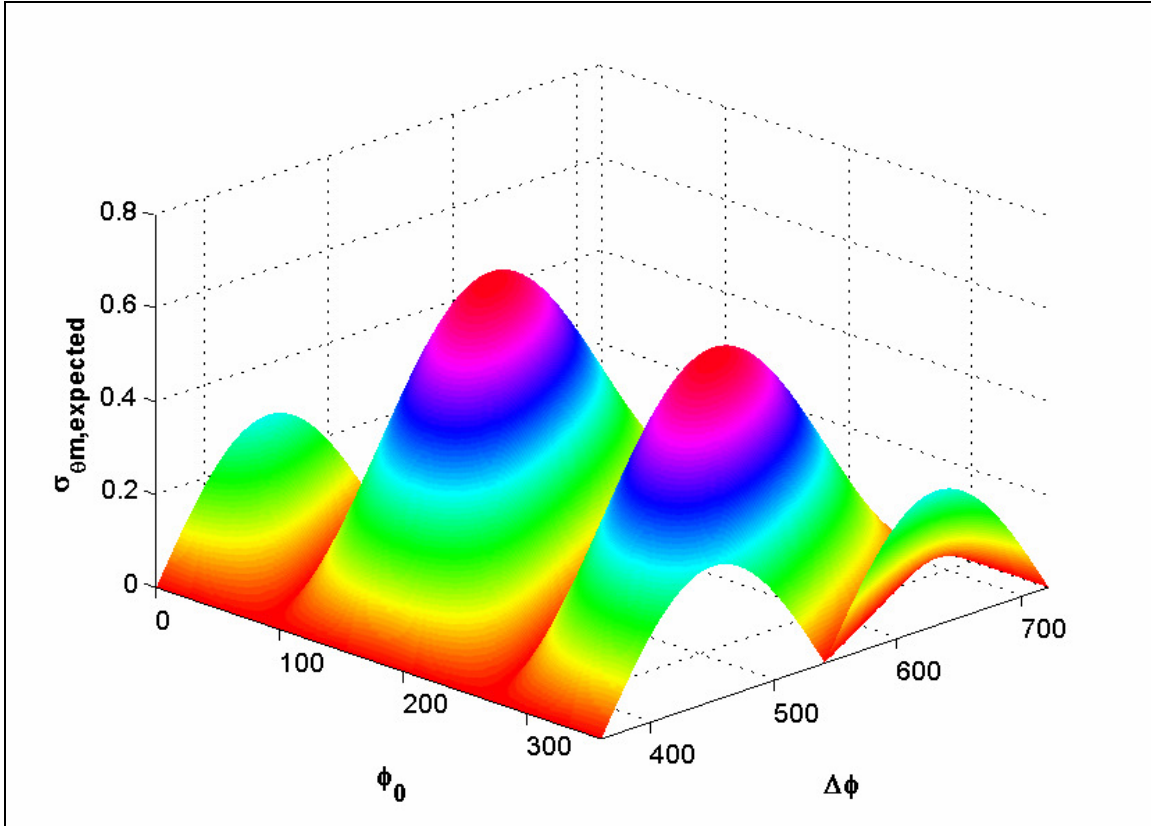


**Figure 4. Standard Deviation of the Expected Deviation Angle for Interpolated Rates**

## Intermediate Rate Cadence

The most interesting cases arise when the rate cadence is similar to the vibration period. Such cases were studied in the range of rate cadences from 0.1 to 10 times the vibration period. For each value of cadence, the measured and expected displacements were calculated over a large number of vibration cycles ( $\sim 1000$ ). The differences between measured and expected displacements were calculated and the standard deviation of these differences saved. It was verified that neither the phase of the first rate measurement, nor changes in the number of cycles affected the results significantly except in the case of resonance as described below. Any influence from the initial phase is thoroughly averaged out by the large number of measurements and cycles. The resulting standard deviations are shown in Figure 5.

Figure 5 presents several interesting features:

- When the rates are calculated by interpolation
  - The standard deviation of the pseudonoise increases with increasing rate measurement cadence until a cadence of about 1, at which point it has a value equal to the amplitude of the vibration.
  - At cadences above 1, the standard deviation of the pseudonoise oscillates with rate measurement cadence between 1 and roughly 0.8 times the amplitude of the vibration.
- When the rates are calculated by extrapolation
  - The standard deviation of the pseudonoise increases with increasing rate measurement cadence until a cadence of about 0.57, at which it has a value equal to roughly 1.82 times the amplitude of the vibration.
  - At cadences above 0.57, the standard deviation of the pseudonoise oscillates with rate measurement cadence between 1 and roughly 1.7 times the amplitude of the vibration. The minima of this oscillation match in cadence and standard deviation the maxima of the oscillations for interpolated values.
- For both interpolation and extrapolation, the standard deviations form a smooth curve except at resonance conditions. This smooth curve approaches a standard deviation of 1 as the rate cadence approaches integer values. When the ratio of the vibration frequency to the cadence is exactly an integer multiple of 0.5, the standard deviation of the pseudonoise jumps to  $1/\sqrt{2}$ . These singular points are due to resonances and are discussed below.

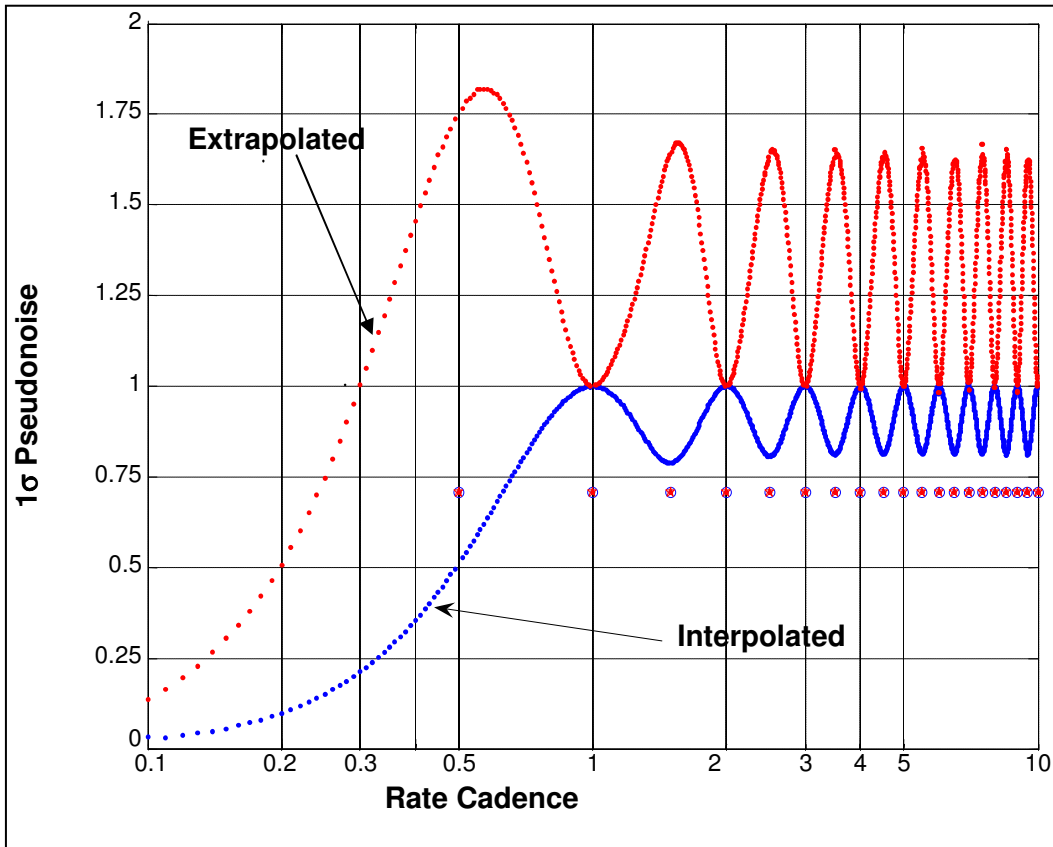


**Figure 5. Pseudonoise as a Function of Rate Measurement Cadence**

## RESONANCES

When the rate or sensor measurements are regularly spaced with respect to the vibration frequency, measurement standard deviations exhibit quite different patterns. Under these resonant conditions the apparent noise depends strongly on initial measurement phase.

### Rate Measurement Cadence

When the rate measurement cadence is an integer multiple of  $\frac{1}{2}$  the vibration frequency in the one dimensional simulation, the pseudonoise exhibits unusual behavior. This behavior can be attributed to a resonance between the vibration frequency and the rate cadence. The resonance behavior is discussed separately for even and odd half-integer multiples of the frequency.



As described above, the standard deviation of the pseudonoise was found to be  $1/\sqrt{2}$  in these resonant cases. This result is accurate and independent of initial phase for the cases where the rate measurement cadence is an even integer multiple of the half frequency (i.e., an integer multiple of the frequency). This case is illustrated in Figure 6.

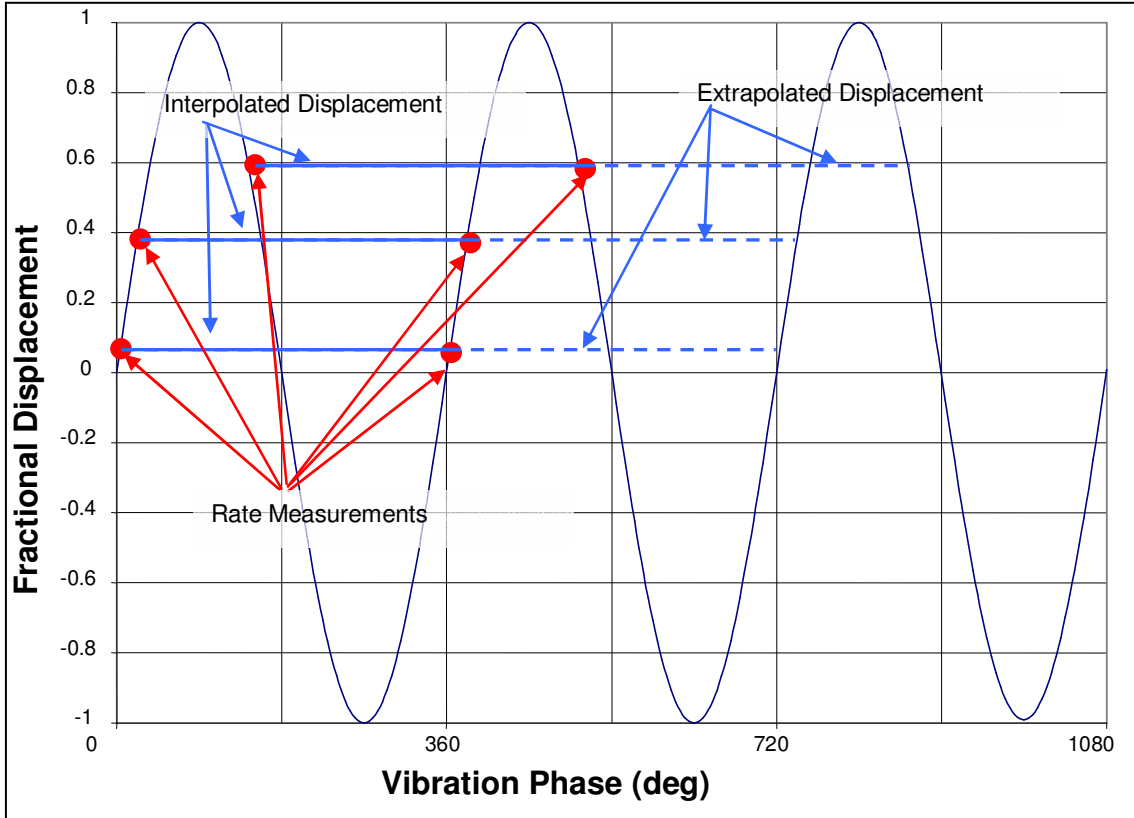


**Figure 6. Calculated Rates for Rate Measurement Cadence Equal to Integer Multiple of Vibration Frequency, Illustrated at Several Initial Phases**

As seen in Figure 6, the rate calculated from rate measurements at cadences that are integer multiples of the vibration frequency is always zero. As a result, the pseudonoise arises only from the sinusoidal variation of the displacement measurements and is independent of the rate measurements.

Next, for cases where the rate measurement cadence is an odd integer multiple of the half frequency, the pseudonoise has different characteristics. This is illustrated in Figure 7.

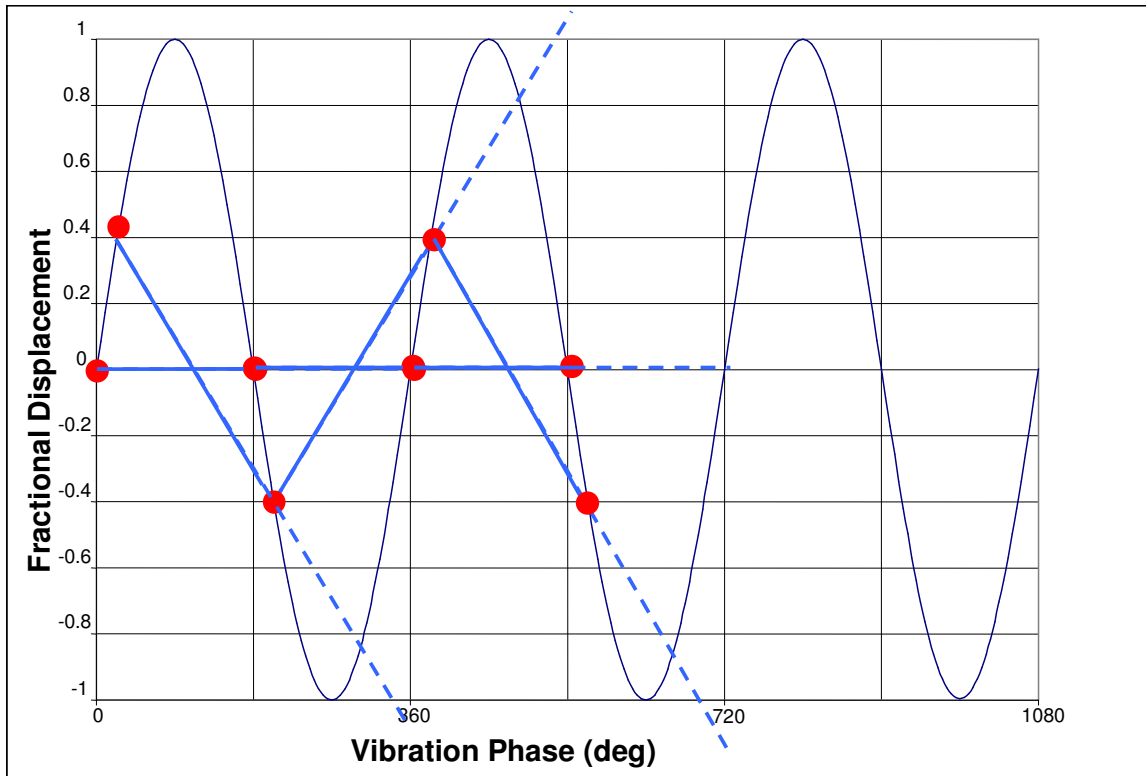


**Figure 7. Calculated Rates for Rate Measurement Cadence Equal to Odd Integer Multiple of Half the Vibration Frequency, Illustrated at Two Initial Phases**  
 (Note: The Labels Used in Previous Figures Have Been Eliminated to Avoid Confusion. The Line Styles and Symbols are Identical to Those in Figure 6.)

When the initial phase is zero, the results are as described above—calculated rates equal to zero and  $1\sigma$  pseudonoise equal to  $1/\sqrt{2}$ . At different initial phases, the calculated rates are not zero and the pseudonoise magnitude varies. Figure 8 shows the pseudonoise standard deviation as a function of initial phase for the case where the rate measurement cadence is exactly half of the vibration frequency.

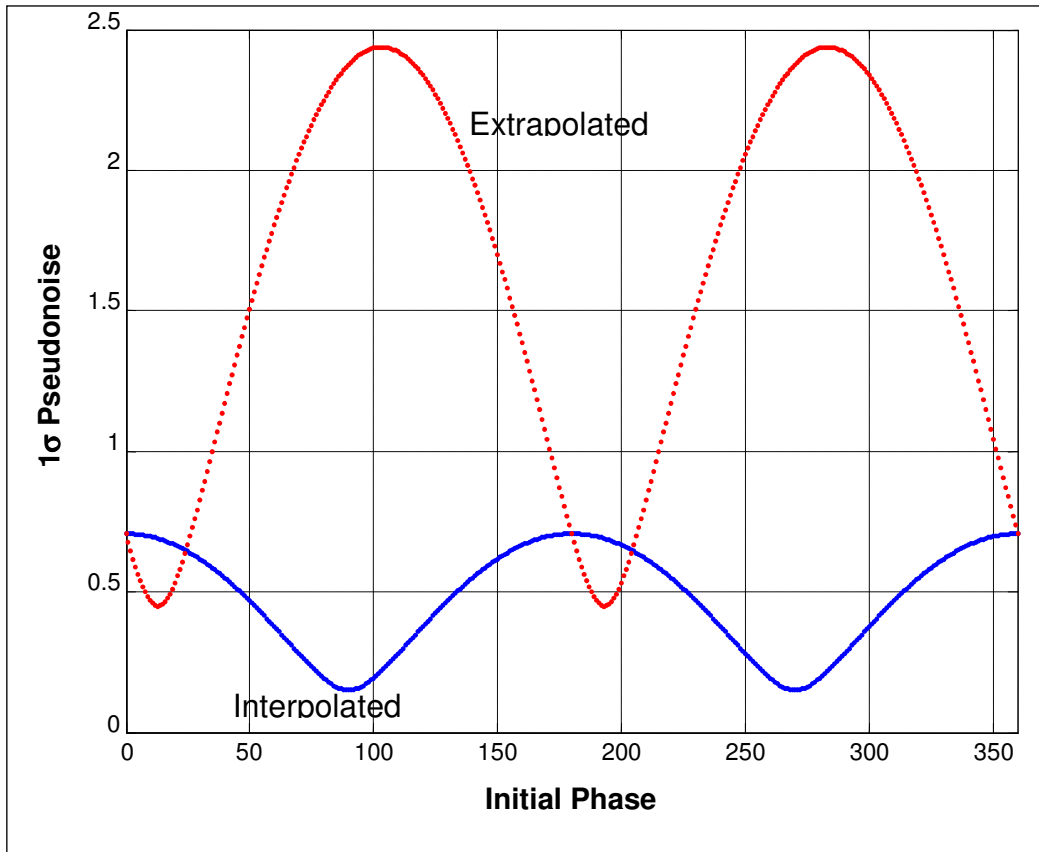


**Figure 8. Pseudonoise Standard Deviation for Rate Measurement Cadence of 0.5, as a Function of Initial Phase**

### Displacement Measurement Cadence

If the displacement measurement cadence is an integer multiple of the vibration frequency, all displacement measurements will be made at the same vibration phase. The mean of the measured displacements will therefore be offset from the mean of the true displacements by an amount corresponding to the vibrational displacement at the time of each displacement measurement. This will result in a systematic error in the displacement measurements.

### Near Resonance Conditions

When either the rate or displacement measurement cadence is near resonance with the vibration frequency, the pseudonoise is similar to cases with exact resonance. The significant difference between exact resonance and near resonance conditions is that in the near resonance conditions the initial phase angle changes slightly in successive cycles whereas the behavior seen in resonance conditions therefore changes gradually with time—it follows the behavior of the resonance conditions with varying initial phase.

## SIMULATIONS

The effect of pseudonoise was evaluated by simulating a system with pseudonoise and evaluating the apparent sensor noise. The software used for evaluation of the pseudonoise

was the Multimission Three-Axis Stabilized Spacecraft (MTASS) Attitude Ground Support System (AGSS). This system has been used operationally on many spacecraft over the last 12 years.

The simulation had the following characteristics:

- **Attitude:** The simulated attitude included a sinusoidal oscillation on one axis, imposed on an otherwise constant attitude. The oscillation was generated by the function:

$$\theta(t) = A \sin(\omega t + \varphi_0) \quad (8)$$

where  $\theta(t)$  is the angular displacement on the axis of oscillation at time  $t$ ,  $t$  is the time,  $A$  is the oscillation amplitude,  $\omega$  is the frequency of oscillation, and  $\varphi_0$  is the phase at time zero. The attitude at time  $t$  is a single axis rotation of  $\theta(t)$ . For example, if the oscillation is about the x-axis:

$$M(t) = \begin{bmatrix} 1 & 0 & 0 \\ 0 & \cos(\theta(t)) & \sin(\theta(t)) \\ 0 & -\sin(\theta(t)) & \cos(\theta(t)) \end{bmatrix} \quad (9)$$

where  $M$  transforms vectors from a geocentric inertial (GCI) frame to the body frame.

- **Amplitude:** The noise statistics are proportional to the amplitude for small amplitudes. Amplitudes on the order of 10-20 arcsec were used.
- **Frequency:** The oscillation frequency was  $\pi/3$  Hertz, where  $t$  is in seconds. This value was chosen because it is irrational and therefore would result in no unintentional resonances.
- **Gyro Cadence:** Two sets of gyro cadences were used and the results combined. The first set was generated so that the base 10 logarithms of the cadences were uniformly spaced between -1 and 1. This provides a logarithmic spacing of cadences between 0.1 and 10. Since the oscillation frequency chosen was irrational, these cadences do not intentionally approach resonance.

The second set of cadences were specifically chosen as the oscillation period multiplied by a number of values. The values ranged from 0.1 to 1 in steps of 0.1 and 1.5 to 10 in steps of 0.5. This second set was expected to be near resonance with the oscillation.

- **Sensor Observations:** Two star trackers were simulated with boresights perpendicular to the axis about which the oscillation was generated and perpendicular to each other. In each tracker, five stars were simulated. The positions of the stars in the GCI frame (reference vectors) were kept constant and the body frame positions (simulated observations) for the stars at time  $t$  were generated by rotating the reference vectors by the attitude at that time.

The results of the simulation are shown for two estimation methods. Figure 9 shows a case where the attitude is determined using a Batch Least-Squares (BLS) estimator. Figure 10 shows a case where the attitude is determined using an Extended Kalman Filter (EKF). For both estimators, observations were propagated using interpolated rates. Identical sensor and

rate data were used for the BLS and EKF estimations. Three hours of data were used with five simulated star observations in each tracker every 2 seconds. In the EKF case, the first 200 seconds of residuals (500 residuals) were omitted in computation of residual statistics to allow filter convergence.

The similarity with the behavior predicted with a simple 1-dimensional model, as in Figure 5, is striking, but certain new observations can be made:

1. The resonances at  $\frac{1}{2}$  integer values seen in Figure 5 do not occur in the simulations. This result is not yet explained.
2. Small, non-zero observation residuals were observed on the non-perturbed axes. These residuals were less than 1 percent of the values on the perturbed axis.
3. Comparison of Figures 9 and 10 indicates that the EKF is more sensitive to near resonance conditions than is the BLS estimator.

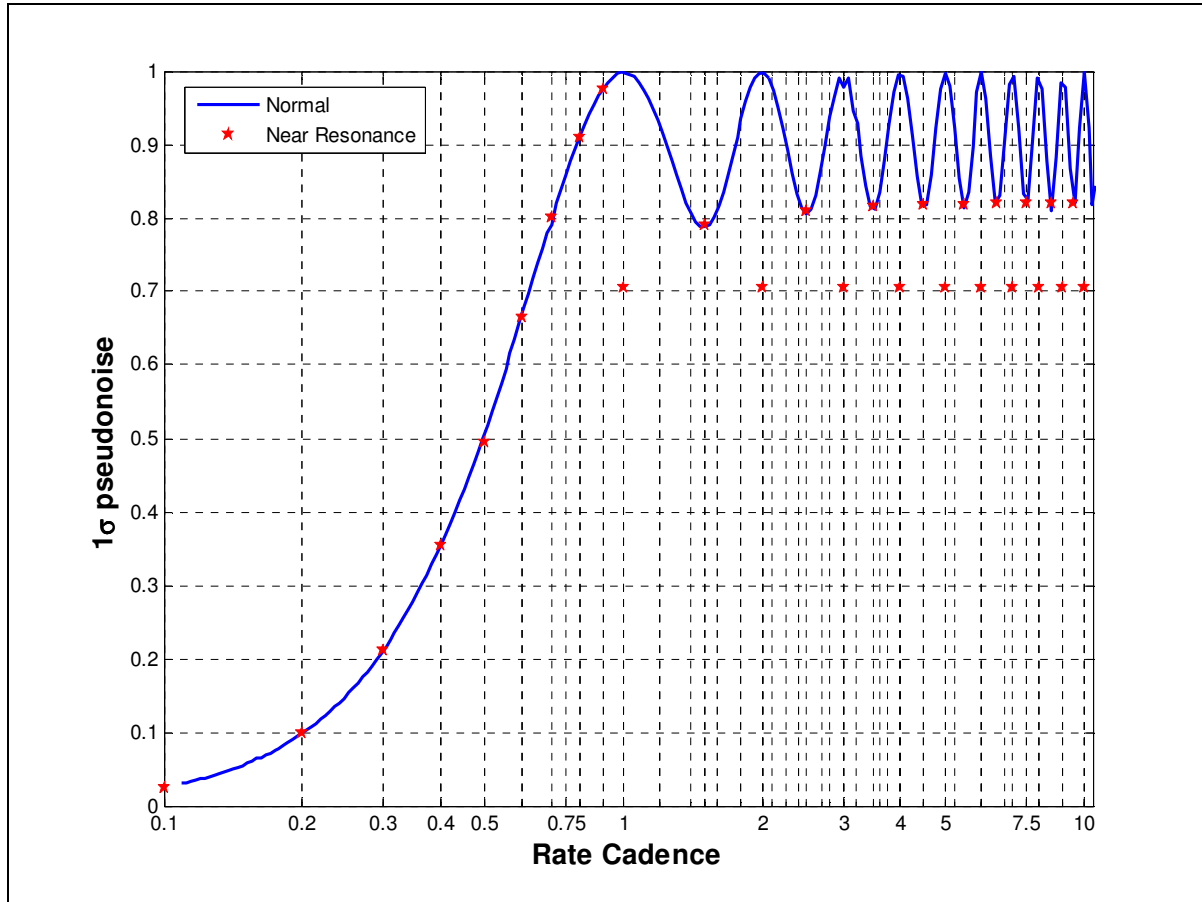


**Figure 9. Results of Batch Least-Squares Simulation of Pseudonoise**

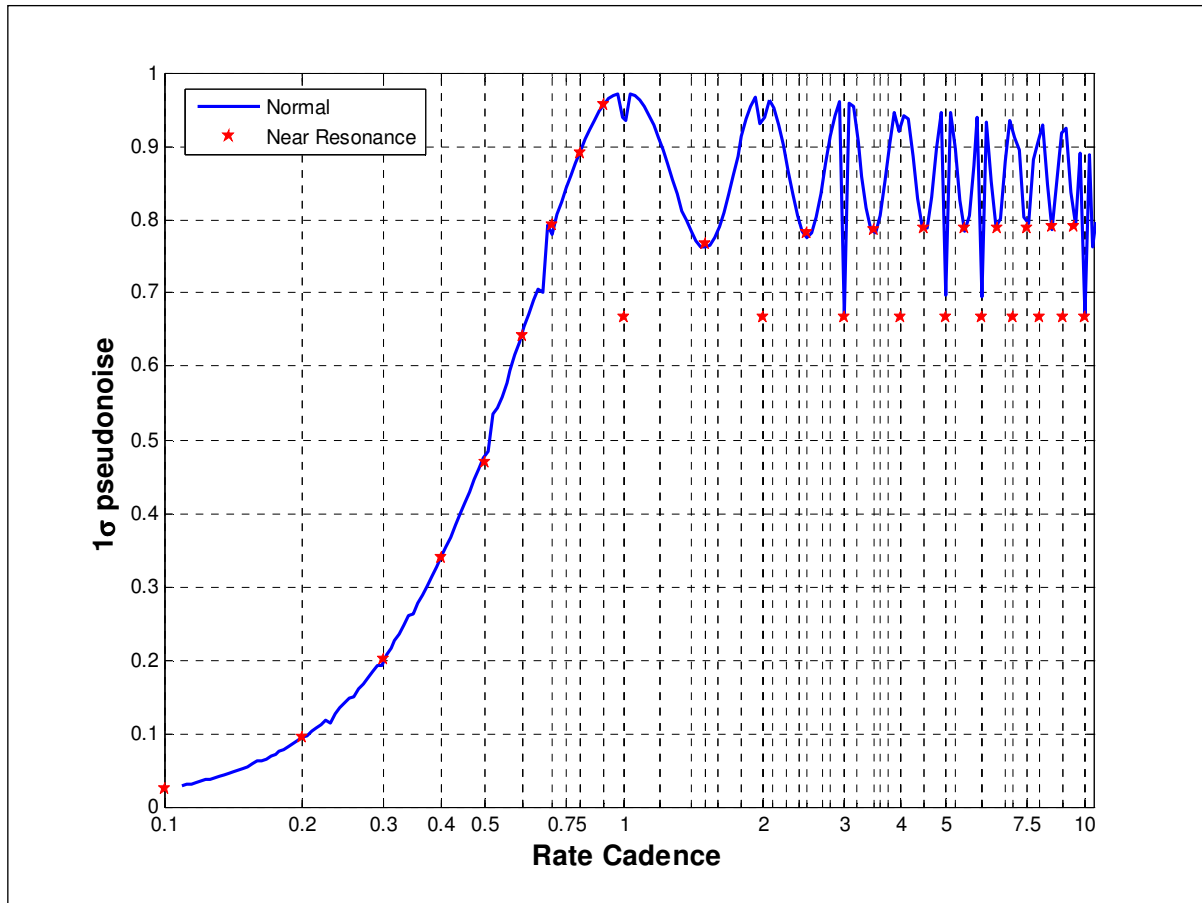


**Figure 10. Results of Extended Kalman Filter Simulation of Pseudonoise (With Interpolated Rates)**

## 5. Conclusions

Pseudonoise is an interesting phenomenon that seldom has a critical impact on attitude determination accuracy. Because pseudonoise generally has zero mean, it may influence the rapidity of filter convergence but will not often significantly influence the accuracy of the converged solution.

Pseudonoise is most important when the rate measurement cadence is comparable to, or larger than, the vibration frequency and when the vibration amplitude is large. Cases where pseudonoise is significant are generally limited by the fact that large amplitude vibrations seldom occur at high frequency because the total vibration energy increases with both frequency and amplitude. Examples of spacecraft having vibrations, rate measurement cadences in the intermediate range described above, and significant vibration amplitudes are Aqua and ADEOS-II. In both of these missions, the apparent star tracker noise was much larger than inherent star tracker noise because of pseudonoise.

Under some conditions, pseudonoise can affect attitude systems and should be considered:

- In cases that are near resonance there are amplified effects that can vary slowly with time.
- In evaluating on-orbit attitude sensor performance, significant portions of apparent sensor error can arise from pseudonoise.
- The observed uncertainty of sensor measurements is a combination of the true sensor measurement uncertainty and the pseudonoise. When the pseudonoise is large, different EKF tuning may be necessary to compute optimal attitudes.